

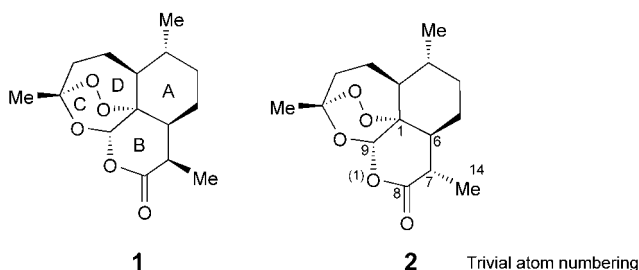
Circular-Dichroism Studies on Artemisinin and Epiartemisinin and Their β -Cyclodextrin Complexes in Solution

by Giancarlo Marconi*, Sandra Monti, Francesco Manoli, Alessandra Degli Esposti, and Andrea Guerrini

Istituto per la Sintesi Organica e la Fotoreattività (ISOF), CNR, via P. Gobetti 101, I-40129 Bologna, Italy
(fax: +39-051-6399844; e-mail: marc@isof.cnr.it)

The circular dichroism (CD) spectra of the powerful antimalarian active principle artemisinin (ART; **1**) from *Artemisia annua*, and of epiartemisinin (EPI, **2**), its C(7) epimer, were studied in solution in the presence and absence of β -cyclodextrin (β -cd). A significant inversion of sign in the region of the second electronic transition was detected. The rotational strengths were successfully calculated within the time-dependent density functional theory (DFT), which enabled us to establish a correlation between the molecular recognition and the biological activities of the two isomers.

1. Introduction. – Recent efforts to find effective drugs to fight malaria, one of the most-deadly human infections, have focused on the marvellous herb *Artemisia annua* and its active principle, artemisinin (= (3R,5aS,6R,8aS,9R,12S,12aR)-octahydro-3,6,9-trimethyl-12H-pyrano[4,3-j]-1,2-benzodioxepin-10(3H)-one; ART; **1**) [1]. ART is an especially powerful antimalarial drug, since the lethal agent, the *Plasmodium falciparum* protozoon, has, so far, not become resistant, at variance with other commonly used drugs such as those based on isoquinolines, e.g., *chloroquine* and *mefloquine*. ART is a sesquiterpene lactone with a characteristic trioxane ring *C* that is crucial for the bioactivity of the compound. Actually, however, the main feature of ART is an endoperoxide (C–O–O–C) function enclosed in the trioxane ring, which is fused to three more rings: a δ -lactone, a cyclohexane, and an oxepane (rings *B*, *A*, and *D*, resp.).



It has been established that the pharmaceutically active part of ART (**1**) comprises the peroxide function of the trioxane ring *C*, along with the lactone ring *B*. The rings *D* and *A* seem to play only a minor or indirect (i.e., structurally organizing) role with respect to the biological properties of the compound [2]. The presence of seven

stereogenic centers makes ART difficult to synthesize in enantiomerically pure form and in sizeable quantities [3]. Moreover, the molecular recognition of ART by the substrate depends critically on relatively small structural changes, as shown by a dramatically reduced activity of the C(7)-epimer¹⁾, epiartemisinin (EPI; **2**) [4]. The subtle relationship between three-dimensional structure and biological activity has recently been demonstrated also for a series of synthetic trioxane-type ART mimicks [5].

Upon treatment of **1** with 1,8-diazabicyclo[5.4.0]undec-7-ene (DBU) in MeCN, one obtains a mixture of **1/2** of ca. 60:40. Thereby, the epimerized form **2** is characterized by an inversion of the configuration at C(7), with the Me group now being in axial α -position. Previous studies [4] have shown that EPI is four-to-seven-times less active than ART due to the structural differences between the two compounds. In particular, the X-ray crystal structure of EPI showed that 1) the α -Me group at C(7), i.e., Me(14), acts as a switch due to steric hindrance, and 2) that the lactone ring *B* undergoes a large structural change, in contrast to the trioxane part (the pharmacophore), which is structurally hardly affected.

In this paper, we examine the consequences brought about by the epimerization at C(7) on the chiroptical and biological-recognition properties of ART.

2. Experimental. – 2.1. *Circular-Dichroism Titrations.* Starting from commercially available artemisinin (Aldrich), the epimer **2** was obtained as described in [4]. The solubility of ART (**1**) in H₂O is rather poor (ca. 4.3×10^{-3} M at 37°), and that of EPI (**2**) is even lower. However, as reported with ART [6], EPI can be dissolved easily up to concentrations of ca. 10^{-3} M at 22° in the presence of a 10^{-2} M soln. of β -cyclodextrin (β -cd). The complexation was, therefore, studied by titrating an aq. 10^{-2} M β -cd soln. with EPI (5×10^{-6} to 1×10^{-3} M). A 10^{-3} M soln. of EPI in Et₂O was prepared, precise aliquots were introduced in suitable flasks, and the solvent was evaporated. Then, known volumes of the β -cd stock soln. were added. After stirring and equilibration, CD spectra were taken. For anal. purposes, the β -cd signal was subtracted from the total signal, and the difference was attributed to contributions of EPI. The spectral data were analyzed by a global-analysis procedure based on the SPECFIT32 commercial program, which determines the best complexation model (stoichiometry) and the association constants (K_a).

2.2. *Computational Methods.* All calculations were performed with the GAUSSIAN-03 software package [7], which determines CD spectra by taking advantage of the recent protocol implemented by Autschbach *et al.* [8] to estimate the rotational strengths (ellipticities). The ground-state geometries of ART and EPI were optimized by means of the B3LYP/6-31G* method [9–11], starting from the X-ray crystal coordinates of ART [4] and EPI [12] as the initial geometries. Previous studies based on the same density-functional-theory (DFT) method have shown that this prediction provides reliable geometric properties of ART and related model trioxanes [13][14].

The excited-state properties such as oscillator and rotational strengths were calculated both in the dipole-length and the dipole-velocity frameworks with the TDDFT method [15][16], using the 6-31 + G* basis set [17] and the B3LYP hybrid functional. The latter was shown to give reliable results for the low-lying excited states of a series of different chromophores [18]. The relevant rotatory strengths are expressed in the dipole-length and the dipole-velocity schemes by *Eqns. 1* and 2, respectively:

$$R_{0i}^r = \frac{1}{2c} \langle \Psi_0 | \hat{r} \times \hat{\nabla} | \Psi_i \rangle \langle \Psi_0 | \hat{r} | \Psi_i \rangle \quad (1)$$

$$R_{0i}^v = \frac{1}{2cE_{0i}} \langle \Psi_0 | \hat{r} \times \hat{\nabla} | \Psi_i \rangle \langle \Psi_0 | \hat{\nabla} | \Psi_i \rangle \quad (2)$$

¹⁾ Trivial atom numbering according to the chemical formulae shown.

Recently a systematic investigation of modern quantum-chemical methods to predict electronic CD spectra [18] has shown that, although the velocity form (Eqn. 2) is gauge-invariant, the formulation in Eqn. 1 generally provides better results. Therefore, the results obtained by the latter formalism will be presented. The CD spectra were simulated by means of a sum of Gaussians centered on the transition wavelengths of the relevant excited states i according to Eqn. 3 [19]:

$$\Delta\epsilon(E) = \frac{1}{2.297 \times 10^{-39}} \frac{1}{\sqrt{2\pi}\sigma} \sum_i^A \Delta E_i R_i e^{[-(E-\Delta E_i)^2/2\sigma^2]} \quad (3)$$

where $\sigma\sqrt{2}$ represents the bandwidth, and ΔE_i and R_i are the excitation energies and the rotatory strengths for the i -th transition, respectively. The graphic program Molden [20] was used to draw the pictures of the molecular orbitals involved in the lowest excited states (see Fig. 5, below).

3. Results and Discussion. – **3.1. CD and UV/VIS Spectra.** The absorption spectra of ART (1) and EPI (2) in H₂O or in EtOH in the absence or presence of β -cyclodextrin (β -cd) (10^{-2} M) are shown in Fig. 1. The two spectra recorded in EtOH in the presence of β -cd appear rather similar, both being characterized by an intense absorption band with a maximum below 200 nm (not accessible), a shoulder at 220–230 nm (much more evident in EPI, though), and a tail extending above 300 nm. The spectrum of EPI proper in EtOH, recorded at higher concentration, more clearly shows the lowest-energy absorption band, extending up to 350 nm. The CD spectrum of ART was already described in [6].

In Fig. 2, the relative CD signals obtained from a series of samples at different EPI concentrations in the presence of β -cd (10^{-2} M) are shown. The signals vary in intensity with increasing EPI concentration, but the principal shape is maintained during the titration. The CD signals, positive below 200 nm, show a well-defined positive band with a maximum at *ca.* 214 nm and a positive tail extending up to *ca.* 320 nm. Global analysis suggested a 1:1 association complex, with a $\log K_a$ value of 2.4 ± 0.4 at 22°.

The absolute CD spectrum of the above EPI/ β -cd complex is represented in Fig. 3, together with the corresponding spectrum of the ART/ β -cd complex [6] and the absolute CD spectrum of EPI in EtOH. By comparing these spectra, it is worth noting that the λ_{\max} value of 214 nm of the positive band of the EPI complex does not coincide with that at 230 nm of the negative band of the ART complex [6]. Moreover, the calculated differential extinction coefficient in the EPI complex ($\Delta\epsilon = 4 \text{ M}^{-1} \text{ cm}^{-1}$ at 214 nm) is similar to that of EPI in EtOH ($3.3 \text{ M}^{-1} \text{ cm}^{-1}$ at 218 nm). These features point to an 'ethanolic' environment for EPI in the β -cd cavity, consistent with a location close to the primary rim of the host.

3.2. Calculated Geometries. The dihedral angles calculated for the optimized geometries of the two compounds within the isolated molecule model generally agreed with those of the X-ray crystal structures [4][12] within 2° for all the rings, with the exception of the lactone *B*-ring. Indeed, it has been stressed earlier [4] that the main structural difference between ART and EPI is reflected in the *B*-ring. It appears that, in the solid state, the lactone ring, which in ART assumes a half-chair, tends to adopt an envelope conformation in EPI, while the rings *A*, *C*, and *D* retain their conformations.

The calculated and X-ray intra-annular torsional angles of the lactone ring of both ART and EPI are collected in Table 1. The much shorter distance between Me(14) and the peroxide function, 4.657 vs. 3.585 Å for ART vs. EPI, respectively, leads to an

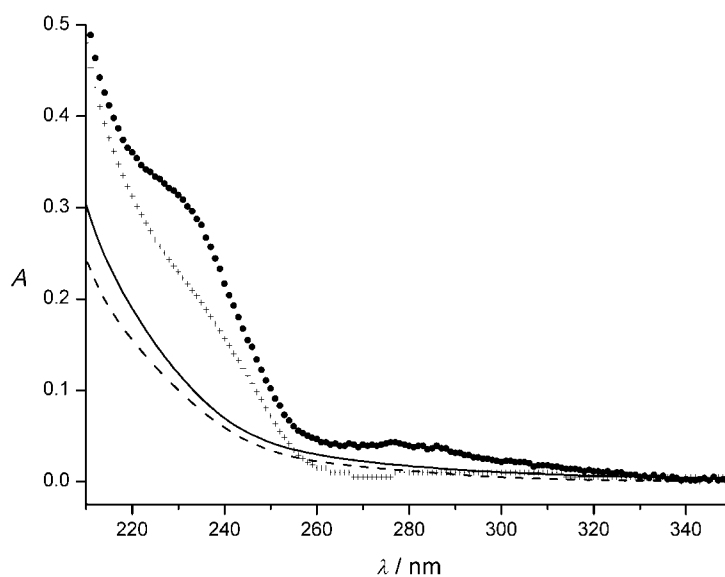


Fig. 1. UV/VIS Absorption spectra of plain EPI (**2**) in EtOH (••••), of EPI/ β -cyclodextrin in H_2O (++++), of plain ART (**1**) in EtOH (----), and of ART/ β -cyclodextrin in H_2O (—). The spectra recorded in the presence of β -cyclodextrin (β -cd) were referenced to the plain β -cd solution. Conditions: 1-cm quartz cuvette, $T = 295\text{ K}$; concentrations: $[EPI] = 1.26\text{ mM}$, $[ART] = 1.01\text{ mM}$, $[\beta\text{-cd}] = 10\text{ mM}$.

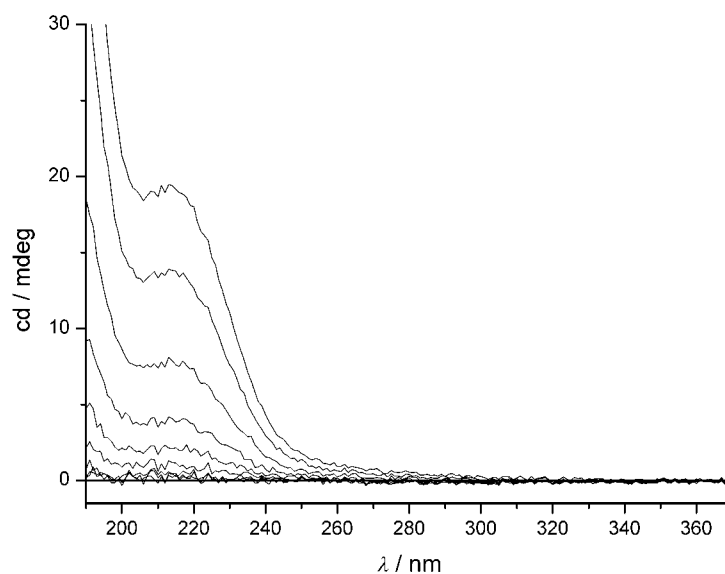


Fig. 2. CD Titration of β -cyclodextrin in H_2O with EPI (**2**). Conditions: 0.2-cm quartz cuvette, $T = 295\text{ K}$; concentrations: $[\beta\text{-cyclodextrin}] = 1 \times 10^{-2}\text{ M}$, $[EPI] = 5 \times 10^{-6}, 1 \times 10^{-5}, 2 \times 10^{-5}, 5 \times 10^{-5}, 1 \times 10^{-4}, 2 \times 10^{-4}, 4 \times 10^{-4}, 7 \times 10^{-4}, \text{ and } 1 \times 10^{-3}\text{ M}$. The β -cyclodextrin spectrum was subtracted in each case.

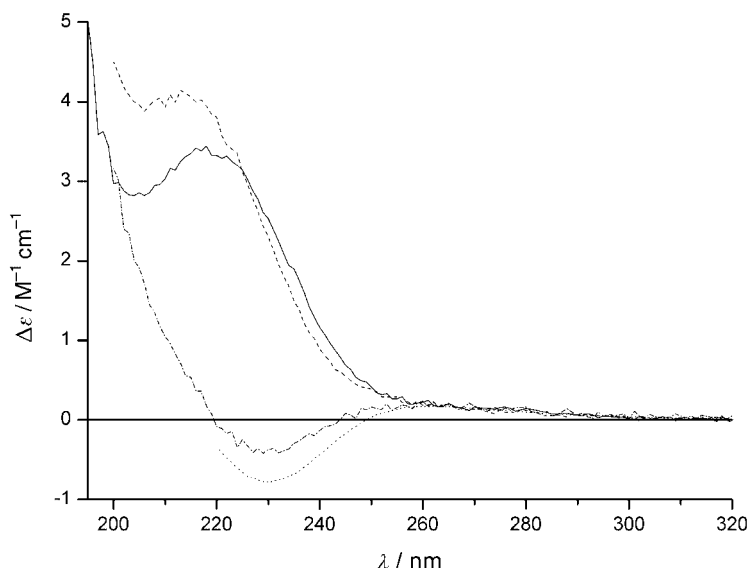


Fig. 3. CD Spectra of EtOH solutions of plain ART (.....) and EPI (—), and of aqueous solutions of the complexes ART/ β -cyclodextrin (– · – · –) and EPI/ β -cyclodextrin (-----), respectively

increased steric hindrance between these two groups in the latter. Thus, EPI is slightly less stable, its calculated overall energy being higher by 1.15 kcal/mol relative to ART.

Table 1. Comparison of Calculated vs. Experimental (X-ray crystal structures) dihedral angles τ for the lactone ring B of Artemisinin (ART; **1** [4]) and Epi-Artemisinin (EPI; **2** [12])

τ [°] ¹⁾	1 (X-ray)	1 (calc.)	2 (X-ray)	2 (calc.)
C(9)–C(1)–C(6)–C(7)	59.0	56.7	54.2(5)	54.0
C(1)–C(6)–C(7)–C(8)	–50.8	–51.8	–25.9(6)	–28.6
C(6)–C(7)–C(8)–O(1)	28.4	32.6	–9.2(7)	–5.3
C(7)–C(8)–O(1)–C(9)	–14.4	–18.9	15.8(7)	14.1
C(8)–O(1)–C(9)–C(1)	22.7	24.5	14.6(6)	13.0
O(1)–C(9)–C(1)–C(6)	–44.8	–43.1	–49.0(5)	–47.1

3.3. Calculated Circular-Dichroism Spectra. The calculated rotational strengths R of the lowest-excited *singlet* states of ART and EPI are reported in Table 2, together with the corresponding absorption wavelengths λ , oscillator strengths f , and magnetic-dipole transition moments m . In Fig. 4, the simulated spectra of ART and EPI in the 200-to-250-nm region are also reported. It is worth noting that the EPI band is blue-shifted relative to that of ART, in agreement with the experiment.

Upon comparing the oscillator strengths with the values of the transition magnetic-dipole moments in Table 2, the relatively large CD values with respect to the absorption signal can be rationalized. In fact, the two lowest *singlet* states of both isomers mainly derive from promotions of highest-occupied (HOMO) to lowest-virtual molecular orbitals, which have large participations of the n orbitals centered on the peroxide and

C=O O-atoms, with intrinsically large transition magnetic-dipole moments m . The product of m times the weak (but nonzero) *electric* transition moment gives rise to the actual CD signals (*Fig. 3*), which, thanks to the different signs, provide more-detailed informations on the excited states of the two compounds than the UV/VIS absorption characteristics (*Fig. 1*).

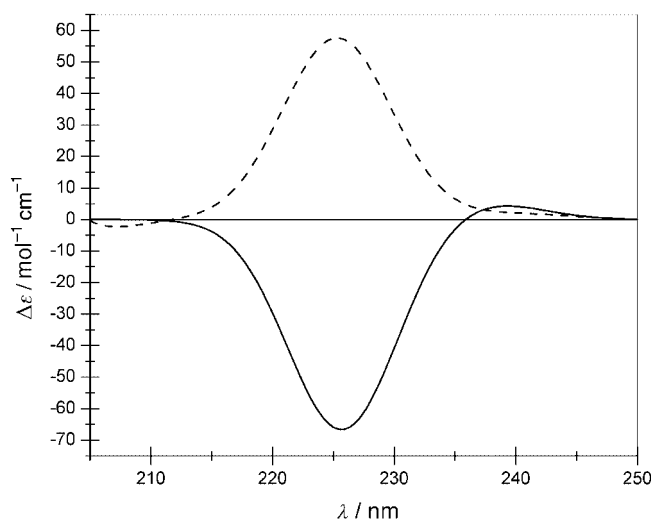


Fig. 4. Simulated CD spectra of ART (**1**; solid line) and EPI (**2**; dotted line) in the region 205–250 nm. For details, see text and *Experimental*.

When comparing the relative electronic compositions of the lowest excited states of ART vs. EPI (last column in *Table 2*), it appears that the structural changes described in the previous section also lead to meaningful differences in the electronic distribution of the two molecules not only in the ground state. Particularly striking is the origin of the CD signal in EPI for the second transition, arising from the combination of four almost equivalent configurations, while just two equivalent electron promotions are described for ART.

It is also interesting to compare the different electronic distributions of the highest-occupied and the lowest-virtual orbitals of the two compounds. In *Fig. 5*, the shape of the HOMO–1, HOMO, LUMO, and LUMO+1 orbitals for ART and EPI, respectively, are shown. One can clearly see the different space distributions of HOMO and HOMO–1 contributing to the lowest *singlet* state (S_1). With respect to the peroxide function, we observe that the S_1 wavefunction in ART shows a fairly delocalized charge distribution, with contributions of the n orbitals of both the peroxide and the C=O O-atoms. In contrast, the peroxide bond is largely localized on the HOMO in the case of EPI.

The above features open up the possibility to gain insight into the different chemical behaviors of the two compounds. In fact, although the S_1 states are calculated to have the same energy, the shape of the potential-energy curve relevant to the dissociation of the peroxide O–O bond is certainly dependent on a local promotion of the type

Table 2. *Calculated CD Wavelengths (λ , in nm), Oscillator Strengths (f), Rotational Strengths (R , in 10^{-40} erg-esu-cm/Gauss), Components of the Transition Magnetic-Dipole Moment (m , in a.u.), and Compositions of the Five Lowest Excited Singlet States of Artemisinin (**1**) and Epi-Artemisinin (**2**)*

	λ	$f \times 10^{-3}$	R	m_x, m_y, m_z	Composition ^{a)}
Artemisinin:					
S ₁	237.5	0.3	0.5825	0.1076, 0.1146, 0.0911	0.39 (H – 1/L) 0.47 (H/L)
S ₂	225.7	0.7	– 7.6281	0.7793, 0.4614, 0.2453	0.36 (H – 2/L + 1) – 0.36 (H – 1/L + 1)
S ₃	199.5	1.0	– 2.9534	0.0890, 0.1138, – 0.0879	0.49 (H – 1/L) – 0.41 (H/L)
S ₄	195.9	3.5	9.1716	0.1980, – 0.3423, 0.1397	0.44 (H – 1/L) 0.47 (H/L + 1)
S ₅	192.8	10	9.8804	– 0.2607, – 0.1734, – 0.6772	0.57 (H – 2/L)
Epi-Artemisinin:					
S ₁	239.9	0.3	0.1984	0.1346, – 0.0282, – 0.0828	0.55 (H/L) – 0.30 (H/L + 1)
S ₂	225.3	0.5	6.5927	0.8781, – 0.1072, – 0.1847	0.37 (H – 1/L + 2) – 0.34 (H – 1/L + 1) – 0.26 (H – 1/L) – 0.27 (H – 1/L + 4)
S ₃	196.1	6.5	– 1.6576	0.1353, – 0.0178, 0.0545	0.59 (H – 1/L) – 0.31 (H – 1/L + 1)
S ₄	192.9	2.4	8.0377	– 0.1513, – 0.0193, 0.1627	0.55 (H/L + 1) 0.27 (H/L) 0.26 (H/L + 2)
S ₅	191.5	12	12.6694	– 0.2670, 0.1205, 0.7220	0.53 (H – 2/L) – 0.24 (H – 3/L)

^{a)} The characters 'H' and 'L' denote HOMO (highest-occupied) and LUMO (lowest-unoccupied molecular orbital), resp.

$\sigma(\text{O}=\text{O}) \rightarrow \sigma^*(\text{O}=\text{O})$ with respect to a more-delocalized promotion of the type $n(\text{C}=\text{O}) \rightarrow \sigma^*(\text{O}=\text{O})$. This difference can be reflected in a different velocity of, say, an electron transfer. Therefore, the structural differences brought about by the simple inversion at C(7) are the cause of significant alterations not only of the molecular ground-state geometry, but also of the properties and electronic distributions of the excited states. As a consequence, dramatic differences are observed with respect to both the chemical and biological activities of ART and EPI.

Recently, there has been a lively debate on the observation that the *biological* activity of ART (**1**) does not correlate with its *chemical* reactivity [21]. The initial idea of oxidative stress induced by the radical produced by dissociative reduction of the O–O bond has been questioned in favor of formation of a more-specific drug/substrate complex. Also, the hypothesis of inhibition of the polymerization of heme to form hemozoin in the food vacuole of the malaria parasite has been argued [22][23]. The observation that structural changes involving a ring remote from the pharmacologically active part of ART, such as that brought about by epimerisation at C(7), reduces significantly the biological activity of ART, points decidedly to the formation of a specific initial ART/substrate complex, rather than to the direct formation of a distonic

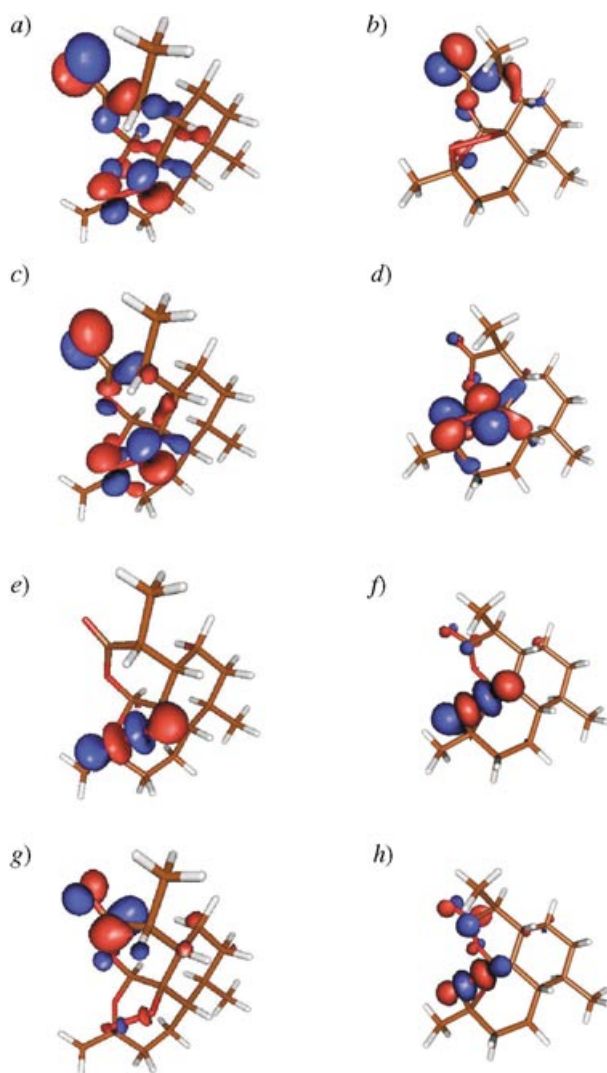


Fig. 5. Shapes of the *HOMO* – 1, *HOMO*, *LUMO*, and *LUMO* + 1 orbitals of ART (a, c, e, g) and EPI (b, d, f, h, resp.)

radical²⁾ in the free compound, as previously hypothesized [24]. This new view is not in contrast with the results obtained from the study of β -cd inclusion of ART. In fact, while biochemical studies [25] have stressed an enhanced bioavailability of ART when administered to β -cd (especially due to increased solubility), structural studies have

²⁾ The unpaired electron was assumed to be centered first on the O–O moiety, and then to move to a C-atom.

shown that the O–O moiety is not fully introduced into the cavity of the macrocycle [6].

The interaction of EPI with β -cd, however, points to a deeper inclusion of this isomer, with an optical activity exalted by complexation. Although no data are available for the biological activity of the EPI/ β -cd complex, the results presented here seem to corroborate the hypothesis that the peroxide moiety by itself is not sufficient to explain the pharmacological activity of ART, and that the molecule must be considered as a whole to elucidate its extraordinary antimalarian power. Since circular dichroism is particularly suitable to study molecular inclusion complexations of various substrates with cyclodextrins (and other hosts) due to its sensitivity to relatively small structural changes, we think that chiroptical examination of the inclusion of ART in biologically mimicking substrates such as nanoparticles and vesicles will be of great interest.

4. Conclusions. – A detailed structural and chiroptical comparison of artemisinin (ART, **1**) and its C(7)-epimer, epiartemisinin (EPI, **2**), has been made to rationalize the main features of the CD spectra of these compounds. The most-important difference in the CD spectra is due to a sign inversion in the region of the second transition, giving rise to a specular signal reminiscent of the spectrum of the enantiomer. From the geometric and electronic structures, it appears that the different chemical behavior of EPI with respect to ART is related to both the inversion of the C(7) stereocenter and the altered conformation of the lactone ring *B*. The latter assumes an envelope structure in EPI to minimize the steric hindrance brought about by the shorter distance between Me(14) and the peroxide moiety. This geometrical change appears particularly relevant for the recognition of the drug by the associating substrate and gives a hint on the mechanism of action of this powerful antimalarian drug. Moreover, it renders questionable the efforts to produce more-soluble compounds by substituting the Me(14) group by more-hydrophilic, but sterically unfavorable, groups. Future studies carried out with ART and its derivatives or analogs are presumed to be of great importance to unravel the mechanism of action of this important compound.

REFERENCES

- [1] R. K. Haynes, S. C. Vonwiller, *Acc. Chem. Res.* **1997**, *30*, 73.
- [2] R. K. Haynes, S. C. Vonwiller, *Tetrahedron Lett.* **1996**, *37*, 253; K. Haynes, S. C. Vonwiller, *Tetrahedron Lett.* **1996**, *37*, 257.
- [3] G. Schmid, W. Hofheinz, *J. Am. Chem. Soc.* **1983**, *105*, 624.
- [4] C. W. Jefford, U. Burger, P. Millasson-Schmidt, G. Bernardinelli, B. L. Robinson, W. Peters, *Helv. Chim. Acta* **2000**, *83*, 1239.
- [5] J. Cazelles, A. Robert, B. Meunier, *J. Org. Chem.* **2002**, *67*, 609.
- [6] G. Marconi, S. Monti, F. Manoli, A. Degli Esposti, B. Mayer, *Chem. Phys. Lett.* **2004**, *383*, 566.
- [7] M. J. Frisch, G. W. Trucks, H. B. Schlegel, G. E. Scuseria, M. A. Robb, J. R. Cheeseman, J. A. Montgomery Jr., T. Vreven, K. N. Kudin, J. C. Burant, J. M. Millam, S. S. Iyengar, J. Tomasi, V. Barone, B. Mennucci, M. Cossi, G. Scalmani, N. Rega, G. A. Petersson, H. Nakatsuji, M. Hada, M. Ehara, K. Toyota, R. Fukuda, J. Hasegawa, M. Ishida, T. Nakajima, Y. Honda, O. Kitao, H. Nakai, M. Klene, X. Li, J. E. Knox, H. P. Hratchian, J. B. Cross, C. Adamo, J. Jaramillo, R. Gomperts, R. E. Stratmann, O. Yazyev, A. J. Austin, R. Cammi, C. Pomelli, J. W. Ochterski, P. Y. Ayala, K. Morokuma, G. A. Voth, P. Salvador, J. J. Dannenberg, V. G. Zakrzewski, S. Dapprich, A. D. Daniels, M. C. Strain, O. Farkas, D. K. Malick, A. D. Rabuck, K. Raghavachari, J. B. Foresman, J. V. Ortiz, Q. Cui, A. G. Baboul, S. Clifford, J. Cioslowski, B. B. Stefanov, G. Liu, A. Liashenko, P. Piskorz, I. Komaromi, R. L. Martin, D. J. Fox, T. Keith, M. A. Al-Laham, C. Y. Peng,

- A. Nanayakkara, M. Challacombe, P. M. W. Gill, B. Johnson, W. Chen, M. W. Wong, C. Gonzalez, J. A. Pople, Gaussian 03, Revision B.05, *Gaussian, Inc.*, Pittsburgh, PA, U.S.A., 2003.
- [8] J. Autschbach, T. Ziegler, S. J. A. van Gisbergen, E. J. Baerends, *J. Chem. Phys.* **2002**, *116*, 6930.
- [9] A. D. Becke, *J. Chem. Phys.* **1993**, *98*, 5648.
- [10] P. C. Hariharan, J. A. Pople, *Theor. Chim. Acta* **1973**, *28*, 213.
- [11] M. M. Francl, W. J. Pietro, W. J. Hehre, J. S. Binkley, M. S. Gordon, D. J. DeFree, J. A. Pople, *J. Chem. Phys.* **1982**, *77*, 3654.
- [12] I. Leban, L. Golic, M. Japelj, *Acta Pharm. Jugosl.* **1988**, *38*, 71.
- [13] J. Gu, K. Chen, H. Jiang, J. Leszczynski, *THEOCHEM* **1999**, *491*, 57.
- [14] S. Tonmunphean, S. Irle, S. Kokpol, V. Parasuk, P. Wolschann, *THEOCHEM* **1998**, *454*, 87.
- [15] R. E. Stratmann, G. Scuseria, M. Frisch, *J. Chem. Phys.* **1998**, *109*, 8218.
- [16] R. Bauernschmitt, R. Ahlrichs, *Chem. Phys. Lett.* **1996**, *256*, 454.
- [17] T. Clark, J. Chandrasekhar, P. v. R. Schleyer, *J. Comput. Chem.* **1983**, *4*, 294; R. Krishnam, J. S. Binkley, R. Seeger, J. A. Pople, *J. Chem. Phys.* **1980**, *72*, 650; P. M. W. Gill, B. G. Johnson, J. A. Pople, M. J. Frisch, *Chem. Phys. Lett.* **1992**, *197*, 499.
- [18] C. Diedrich, S. Grimme, *J. Phys. Chem., A* **2003**, *107*, 2524.
- [19] 'Circular Dichroism: Principles and Applications', Eds. K. Nakanishi, N. Berova, R. Woody, Wiley-VCH, New York, Weinheim, 1994.
- [20] G. Schaftenaar, J. H. Noordik, *J. Comput.-Aided Mol. Design* **2000**, *14*, 123.
- [21] R. K. Haynes, W.-Y. Ho, H.-W. Chan, B. Fugmann, J. Stetter, S. L. Croft, L. Vivas, W. Peters, B. L. Robinson, *Angew. Chem., Int. Ed.* **2004**, *116*, 1405.
- [22] U. Eckstein-Ludwig, R. J. Webb, I. D. A. van Goethern, J. M. East, A. G. Lee, M. Kimura, P. M. O'Neill, P. G. Bray, S. A. Ward, S. Krishna, *Nature (London)* **2003**, *424*, 957.
- [23] R. K. Haynes, D. Monti, D. Taramelli, N. Basilico, S. Parapini, P. Olliaro, *Antimicrob. Agents Chemother.* **2003**, *47*, 1175.
- [24] W.-M. Wu, Y. Wu, Y.-L. Wu, Z.-J. Yao, C.-M. Zhou, Y. Li, F. Shan, *J. Am. Chem. Soc.* **1998**, *120*, 3316.
- [25] J. W. Wong, K. H. Yuen, *Int. J. Pharm.* **2001**, *227*, 177.

Received June 24, 2004